

# Deducing the nuclear-matter incompressibility coefficient from data on isoscalar compression modes

S. Shlomo<sup>1</sup>, V.M. Kolomietz<sup>2</sup>, and G. Colò<sup>3,a</sup>

<sup>1</sup> Cyclotron Institute, Texas A&M University, College Station, TX 77843, USA

<sup>2</sup> Institut for Nuclear Research, 03680 Kiev, Ukraine

<sup>3</sup> Dipartimento di Fisica, Università degli Studi, and INFN, via Celoria 16, 20133 Milano, Italy

Received: 15 February 2006 /

Published online: 28 September 2006 – © Società Italiana di Fisica / Springer-Verlag 2006

**Abstract.** Accurate assessment of the value of the incompressibility coefficient,  $K$ , of symmetric nuclear matter, which is directly related to the curvature of the equation of state (EOS), is needed to extend our knowledge of the EOS in the vicinity of the saturation point. We review the current status of  $K$  as determined from experimental data on isoscalar giant monopole and dipole resonances (compression modes) in nuclei, by employing the microscopic theory based on the random-phase approximation (RPA).

**PACS.** 21.65.+f Nuclear matter – 24.30.Cz Giant resonances – 21.60.Jz Hartree-Fock and random-phase approximation

## 1 Introduction

It is well known that the equation of state (EOS),  $E/A = E(\rho)$ , of symmetric nuclear matter (SNM) is a very important ingredient in the study of nuclear properties, heavy-ion collisions, neutron stars and supernovae. Experimentally, we have accurate data on the saturation point of the EOS, namely  $(\rho_0, E(\rho_0))$ . From electron and hadron scattering experiments on nuclei, one finds a constant central density of  $\rho_0 = 0.16 \text{ fm}^{-3}$ , and from the extrapolation of empirical mass formula, we have  $E(\rho_0) = -16 \text{ MeV}$  for SNM. Since at saturation  $\frac{dE}{d\rho}|_{\rho_0} = 0$ , one has

$$E(\rho) = E(\rho_0) + \frac{1}{18}K \left( \frac{\rho - \rho_0}{\rho_0} \right)^2 + \dots, \quad (1)$$

where

$$K = 9\rho_0^2 \frac{d^2(E/A)}{d\rho^2} \Big|_{\rho_0} \quad (2)$$

is the SNM incompressibility coefficient. Therefore, a very accurate value of  $K$  is needed to extend our knowledge of the EOS in the vicinity of the saturation point.

There have been many attempts over the years to determine the value of  $K$  by considering properties of nuclei which are sensitive to a certain extent to  $K$  (see ref. [1]). In a macroscopic approach analysis of experimental data of a certain physical quantity,  $K$  appears in the expression for the physical quantity and the value of  $K$  is determined

by a direct fit to the data. In a microscopic approach, one considers various effective two-body interactions which are associated with different values of  $K$  but reproduce with comparable accuracies the experimental data of various properties of nuclei, such as binding energies and radii. One then determines the effective interaction which best fits the experimental data for a physical quantity which is sensitive to  $K$ . We mention, in particular, the attempts [1–5] of considering as physical quantities: nuclear masses, nuclear radii, nuclear scattering cross-sections, supernova collapses, masses of neutron stars, observables in heavy-ion collisions and the interaction parameters  $F_0$  and  $F_1$  in Landau's Fermi liquid theory for nuclear matter. Here we examine the most sensitive method [6, 7] which is based on experimental data on the strength function distributions of the isoscalar giant monopole resonance (ISGMR),  $T = 0, L = 0$ , and the isoscalar giant dipole resonance (ISGDR),  $T = 0, L = 1$ , which are compression modes of nuclei, analyzed within the microscopic random-phase approximation (RPA) [8].

Over the last three decades, a significant amount of experimental work was carried out to identify strength distributions of the ISGMR and ISGDR in a wide range of nuclei [9–12]. The main experimental tool for studying isoscalar giant resonances is inelastic  $\alpha$ -particle scattering. This is mainly because i)  $\alpha$ -particles are selective as to exciting isoscalar modes, and ii) angular distributions of inelastically scattered  $\alpha$ -particles at small angles are characteristic for some of the multipolar modes. Recent development in the area of experimental investigation of the

<sup>a</sup> e-mail: gianluca.colo@mi.infn.it

isoscalar giant resonances made it possible to measure the centroid energy (that is, the ratio of the energy-weighted and non-energy-weighted sum rules,  $m_1/m_0$ )  $E_0$  of the ISGMR with an error  $\delta E_0 \sim 0.1\text{--}0.3$  MeV [11, 12]. Using the relation  $(\delta K)/K = 2(\delta E_0)/E_0$  and, for example, the recent experimental value of  $E_0 = 13.96 \pm 0.20$  MeV for the ISGMR in  $^{208}\text{Pb}$ , one has an error of  $\delta K = 6\text{--}9$  MeV for  $K = 200\text{--}300$  MeV. This enhanced experimental precision calls for a critical accuracy check of the theoretical calculations. In fact, many available theoretical calculations, in which the monopole centroid is also determined only within about 0.2 MeV, due to various approximations, introduce a further contribution to  $\delta K$  which must be added quadratically to the experimental one, yielding a total error of 8–13 MeV (see [13]).

The extraction of  $K$  from experimental data on ISGMR is not straightforward. There have been several attempts [9] in the past to determine  $K$  simply by a least square fit to the ISGMR data of various sets of nuclei using a semi-empirical expansion in power of  $A^{-1/3}$  of the nucleus incompressibility coefficient,  $K_A$ , obtained from  $E_0$  using, for example, the scaling model assumption (we remind here that in the scaling model a simple shape of the ground-state density  $\rho_0$  is assumed and its changes are associated to a single parameter  $\lambda$ , *i.e.*, they are of the type  $\rho_0 \rightarrow \rho_\lambda(\mathbf{r}) = \frac{1}{\lambda^3} \rho_0(\frac{\mathbf{r}}{\lambda})$ ). It was found [9] that the value deduced for  $K$  varied significantly, depending on the set of data of the ISGMR energies used in the fit. This is mainly due to the limited number of nuclei in which  $E_0$  is known. We also point out that the scaling model assumption is not very reliable for medium and light nuclei.

If we have to resort to theory in order to extract  $K$ , we should start by discussing some principle remarks. The *static* incompressibility coefficient  $K$  of eq. (2) describes the propagation of the *first sound* excitations in nuclear matter having the sound velocity

$$c = c_1 = \sqrt{K/9m}. \quad (3)$$

However, the propagation of the first sound implies the regime of frequent inter-particle collisions [14] which is not realized in cold (and moderately heated) nuclei, where the compression modes are related to the zero sound (rare inter-particle collisions) regime. It is necessary to note that the sound velocity  $c$  and the eigenfrequency  $\omega$  of the compression mode are, in principle, directly related to  $K$  for the first sound mode only. In general, the sound velocity  $c$  is a complicated function of both the incompressibility coefficient  $K$  and the dimensionless collisional parameter  $\omega\tau$ , where  $\omega$  is the frequency of the mode and  $\tau$  is its relaxation time. This complicated dependence is caused by the dynamic distortion of the Fermi surface (FSD) which accompanies the collective motion in a Fermi liquid. In cold nuclear matter, for the rare-collision regime  $\omega\tau \rightarrow \infty$ , one has, instead of eq. (3), the relation

$$c = c_0 = \sqrt{K'/9m}, \quad (4)$$

where  $K'$  is a strongly renormalized incompressibility coefficient which can be shown to obey [15]

$$K' \approx 3K. \quad (5)$$

Thus, within the theory of Fermi liquids, there is a significant difference between the static nuclear incompressibility coefficient,  $K$ , which is defined as the stiffness coefficient with respect to a change in the bulk density, and the dynamic one,  $K'$ , associated with the zero sound velocity and the energy of the ISGMR or ISGDR. Nonetheless, the approximate relation (5) is consistent with the idea that the interaction which best fits the experimental data for ISGMR and ISGDR energies should also provide the correct value of  $K$ .

It can also be shown [15] that the consistent presence of the same FSD effects in the boundary condition strongly suppresses any increase of  $E_0$  (the energy of lowest isoscalar giant monopole resonance) compared to the usual liquid-drop model where the FSD effects are not taken into account. We point out that the FSD effects are completely washed out from the dynamic incompressibility coefficient  $K'$  in the case of the scaling assumption. Note also that the effect of the FSD in the boundary condition is rather small for the overtone excitations. The dynamic and relaxation effects on the ISGMR and on the ISGDR are therefore significantly different. In contrast to the ISGMR, which is the lowest breathing mode, the ISGDR appears as the *overtone* to the lowest isoscalar dipole excitation, which corresponds to a spurious center-of-mass motion. Due to this fact, the energy of the ISGDR,  $E_1$ , varies with  $\tau$  much more than the energy  $E_0$  of the ISGMR.

If one wishes to make a link with microscopic effective interactions, the basic theory for the description of different giant resonance modes is self-consistent Hartree-Fock (HF) plus RPA [6, 8]. The HF calculations using Skyrme-type interactions [16], which are density- and momentum-dependent zero-range interactions, have been very successful in reproducing experimental data on ground-state properties of nuclei. The parameters of the Skyrme interaction are varied so as to reproduce a selected set of experimental data of a wide range of nuclei on nuclear masses, charge and mass density distributions, etc. The nuclear response function is evaluated within RPA, which is a linear response theory suited for the description of small oscillations which can eventually accommodate a proper treatment of the particle continuum [8, 17].

We emphasize that the values of  $E_0$  and  $E_1$  are correlated with the value of  $K$  which is associated with the effective nucleon-nucleon interaction adopted in the HF-RPA calculations, and thus can be used to extract an accurate value for  $K$ . This correlation has been explicitly shown, *e.g.*, in refs. [18, 19].

It is important to point out that the HF-RPA method solves the nuclear effective Hamiltonian in the space of one-particle–one-hole (*1ph*) excitations. Correlations, associated with excitations of *2ph* and higher structures, are not accounted for explicitly. The effects of these correlations have been discussed in the literature, see for example the reviews in refs. [20–22]. The main effect is a collisional broadening of the strength distributions which can be accompanied by a certain shift of the resonance peak position. This shift grows with excitation energy and can be

of the order of 1 MeV for the rather high-lying isovector modes (in the range above 20 MeV). However, in the case of the ISGMR the shift is quite small (of the order of few hundreds of keV [23], that is, comparable with the experimental uncertainty). This is not a numerical accident, rather a consequence of cancellations which arise when all diagrams corresponding to the coupling between  $1ph$  and  $2ph$  states are included (cf. [20] and references therein).

The first experimental identification of the ISGMR in  $^{208}\text{Pb}$  at excitation energy of  $E_0 = 13.7$  MeV [24] already triggered random-phase approximation (RPA) calculations using existing or modified effective interactions: those having  $K = 210 \pm 30$  MeV gave results in agreement with experiment [25]. We point out, however, that i) in the early investigations, the experimental uncertainties for  $E_0$  were relatively large, and only a limited class of effective interactions were explored; ii) many more recent calculations were not fully self-consistent [13, 26]. Consequently, as we will see, we accept nowadays larger values for  $K$ .

The study of the isoscalar giant dipole resonance is very important since this compression mode provides an independent source of information on  $K$ . Early experimental investigation of the ISGDR in  $^{208}\text{Pb}$  resulted in a value of  $E_1 \sim 21$  MeV for the centroid energy [27, 28]. It was first pointed out in ref. [29] that corresponding HF-RPA results for  $E_1$ , obtained with interactions adjusted to reproduce experimental values of  $E_0$ , are higher than the experimental value by more than 3 MeV and thus this discrepancy between theory and experiment raises some doubts concerning the unambiguous extraction of  $K$  from energies of compression modes. A similar result for  $E_1$  in  $^{208}\text{Pb}$  was obtained in more recent experiments [10, 30]. Therefore, the value of  $K$  deduced from these early experimental data on ISGDR is significantly smaller than that deduced from ISGMR data.

Recent relativistic RPA (RRPA) calculations [31, 32], with the inclusion of negative-energy states of the Dirac sea in the response function, yield a value of  $K = 250\text{--}270$  MeV. This result has been obtained using different types of effective Lagrangians, including those having density-dependent coupling constants. Note that since an uncertainty of about 20% in the values of  $K$  is tantamount to an uncertainty of 10% in the value of  $E_0$ , the discrepancy in the value of  $K$  obtained from relativistic and non-relativistic models is quite significant in view of the accuracy of about 2% in the experimental data currently available on the ISGMR centroid energies. In refs. [19, 33] it has been claimed that these significant differences are due to the model dependence of  $K$ . However, in the most recent works of refs. [13, 34, 35] this model dependence has been explained, as we shall discuss.

We should finally point out that it is quite common in theoretical work on giant resonances to calculate the strength function  $S(E)$  for a certain simple scattering operator  $F$ , whereas in the analysis of experimental data of the excitation cross-section  $\sigma(E)$  one carries out distorted-wave Born approximation (DWBA) calculations with a transition potential  $\delta U$  obtained from a collective model transition density  $\rho_{coll}$  using the folding model (FM) ap-

proximation. This may be a source of uncertainties, especially if most of the strength is not collective. Accordingly, it is important to examine the relation between  $S(E)$  and the excitation cross-section  $\sigma(E)$  of the ISGMR and the ISGDR, obtained by  $\alpha$ -scattering, using the folding model DWBA method with  $\rho_t$  obtained from self-consistent HF-RPA.

In sect. 2 we review the basic elements of the microscopic HF-RPA theory for the strength function and the FM-DWBA method for the calculation of the excitation cross-sections of giant resonances by inelastic  $\alpha$ -scattering. In sect. 3, we provide some results of the consequences of violations of self-consistency on the calculated strength function  $S(E)$ , the excitation cross-section  $\sigma(E)$  and recent results of fully self-consistent HF-RPA calculations of the centroid energies ( $E_0$  and  $E_1$ ) for the ISGMR and ISGDR. We also present simple explanations for the discrepancies in the values deduced for  $K$ . Our conclusions are given in sect. 4.

## 2 Formalism

### 2.1 Self-consistent HF-RPA approach

In the microscopic and self-consistent HF-RPA approach, one starts by adopting a specific effective nucleon-nucleon interaction,  $V_{12}$ , and deriving the ground-state mean field. Then, the RPA equations are solved by using the particle-hole ( $p$ - $h$ ) interaction  $V_{ph}$  which is derived from the same mean field determined by  $V_{12}$  (in this sense, the calculation is self-consistent). Various numerical methods have been adopted in the literature to solve the RPA equations, see, for example, refs. [8, 17, 25, 36, 37]. In particular, in Green's function approach [8, 17] one evaluates the RPA Green's function  $G$ , given by  $G = G_0(1 + V_{ph}G_0)^{-1}$ , where  $G_0$  is the free  $p$ - $h$  Green's function. Then, the strength function  $S(E)$  and the transition density  $\rho_t$ , associated with the scattering operator  $F = \sum_{i=1}^A f(\mathbf{r}_i)$ , are obtained from

$$S(E) = \sum_n |\langle 0|F|n\rangle|^2 \delta(E - E_n) = \frac{1}{\pi} \text{Im} [\text{Tr}(fGf)], \quad (6)$$

$$\rho_t(\mathbf{r}, E) = \frac{\Delta E}{\sqrt{S(E)\Delta E}} \int f(\mathbf{r}') \left[ \frac{1}{\pi} \text{Im} G(\mathbf{r}', \mathbf{r}, E) \right] d\mathbf{r}'. \quad (7)$$

Note that  $\rho_t(\mathbf{r}, E)$ , as defined in (7), is associated with the strength in the region of  $E \pm \Delta E/2$ . Green's function approach allows treating the continuum in a proper way. However, the RPA equations can also be solved on a discrete basis. Although the exact solution of RPA in the continuum may be crucial if one treats weakly bound nuclei or if one is interested in the particle decay of states which lie above the threshold, discrete RPA can nonetheless reproduce the main integral properties of giant resonances in stable nuclei.

There are also alternative methods to obtain these integral properties. For instance, the constrained energy

$E_{-1}$  defined as  $\sqrt{m_1/m_{-1}}$ , where  $m_1$  is the energy-weighted sum rule and  $m_{-1}$  is the inverse energy-weighted sum rule, can be calculated once  $m_1$  is extracted from the double commutator  $[F, [H, F]]$  while  $m_{-1}$  is obtained from constrained HF (CHF) calculations [38].

In fully self-consistent HF-RPA calculations, the spurious state (associated with the center-of-mass motion)  $T = 0$ ,  $L = 1$  must appear at zero excitation energy ( $E = 0$ ), aside from small numerical inaccuracies, and no significant spurious state mixing (SSM) in the ISGDR must be expected. However, although not always stated in the literature, many actual implementations of HF-RPA (and relativistic RPA) are not fully self-consistent [26] (see, however, refs. [18, 36, 37, 39–42]). Each approximation introduced in RPA may shift the centroid energies of giant resonances with respect to the exact value, and introduce a SSM in the ISGDR.

In refs. [26, 43, 44], in order to correct for the effects of the SSM on  $S(E)$  and the transition density, the scattering operator  $F = \sum_{i=1}^A f(\mathbf{r}_i)$  has been replaced by the projection operator

$$F_\eta = \sum_{i=1}^A f_\eta(\mathbf{r}_i) = \sum_{i=1}^A f(\mathbf{r}_i) - \eta f_1(\mathbf{r}_i), \quad (8)$$

where  $f(\mathbf{r}) = f(r)Y_{1M}(\Omega)$  and  $f_1(\mathbf{r}) = rY_{1M}(\Omega)$ . The value of  $\eta$  is obtained from the coherent spurious state transition density [45],  $\rho_{ss}(\mathbf{r}) = \alpha_a \frac{\partial \rho_0}{\partial r} Y_{1M}(\Omega)$ , where  $\rho_0$  is the ground-state density of the nucleus. The result for  $f(r) = r^3$  is  $\eta = \frac{5}{3}\langle r^2 \rangle$  [46]. We point out that the ISGDR transition density  $\rho_t$  is obtained [26] from eqs. (7) and (8) after subtracting the spurious state component  $\rho_{ss}$ . In ref. [47] it has been shown that the above procedure is equivalent to project out explicitly the spurious component from each excited state. Further discussions about the SSM can be found in refs. [48, 49].

## 2.2 DWBA calculations of excitation cross-sections

The DWBA has been quite instrumental in providing a theoretical description of low-energy scattering reactions and is widely used in analyzing measured cross-sections of scattered probes. The folding model approach [50] to the evaluation of optical potentials appears to be quite successful and, at present, is extensively used in theoretical descriptions of  $\alpha$ -particle scattering [51]. The main advantage of this approach is that it provides a direct link to the description of  $\alpha$ -particle scattering reactions based on microscopic HF-RPA results.

The DWBA differential cross-section for the excitation of a giant resonance by inelastic  $\alpha$ -scattering is

$$\frac{d\sigma^{DWBA}}{d\Omega} = \left( \frac{\mu}{2\pi\hbar^2} \right)^2 \frac{k_f}{k_i} |T_{fi}|^2, \quad (9)$$

where  $\mu$  is the reduced mass and  $k_i$  and  $k_f$  are the initial and final linear momenta of the  $\alpha$ -nucleus relative motion,

respectively. The transition matrix element  $T_{fi}$  is given by

$$T_{fi} = \left\langle \chi_f^{(-)} \Psi_f | V | \chi_i^{(+)} \Psi_i \right\rangle, \quad (10)$$

where  $V$  is the  $\alpha$ -nucleon interaction,  $\Psi_i$  and  $\Psi_f$  are the initial and final states of the nucleus, and  $\chi_i^{(+)}$  and  $\chi_f^{(-)}$  are the corresponding distorted wave functions of the relative  $\alpha$ -nucleus relative motion, respectively. To calculate  $T_{fi}$ , eq. (10), one can adopt the following approach which is usually employed by experimentalists. First, assuming that  $\Psi_i$  and  $\Psi_f$  are known, the integrals in (10) over the coordinates of the nucleons are carried out to obtain the transition potential  $\delta U \sim \int \Psi_f^* V \Psi_i$ . Second, the cross-section (9) is calculated using a certain DWBA code with  $\delta U$  and the optical potential  $U(r)$  as input.

Within the FM approach, the optical potential  $U(r)$  is given by

$$U(r) = \int d\mathbf{r}' V(|\mathbf{r} - \mathbf{r}'|, \rho_0(r')) \rho_0(r'), \quad (11)$$

where  $V(|\mathbf{r} - \mathbf{r}'|, \rho_0(r'))$  is the  $\alpha$ -nucleon interaction, which is generally complex and density dependent, and  $\rho_0(r')$  is the ground state HF density of a spherical target nucleus. To obtain the results given in the following, both the real and imaginary parts of the  $\alpha$ -nucleon interaction were chosen to have Gaussian forms with density dependence [51], and parameters determined by a fit to the elastic scattering data. The radial form  $\delta U_L(r, E)$  of the transition potential, for a state with the multipolarity  $L$  and excitation energy  $E$ , is obtained from:

$$\delta U(r, E) = \int d\mathbf{r}' \delta \rho_L(\mathbf{r}', E) \left[ V(|\mathbf{r} - \mathbf{r}'|, \rho_0(r')) + \rho_0(r') \frac{\partial V(|\mathbf{r} - \mathbf{r}'|, \rho_0(r'))}{\partial \rho_0(r')} \right], \quad (12)$$

where  $\delta \rho_L(\mathbf{r}', E)$  is the transition density for the considered state.

We point out that within the “microscopic” folding model approach to the  $\alpha$ -nucleus scattering, both  $\rho_0$  and  $\rho_L$ , which enter eqs. (11) and (12), are obtained from the self-consistent HF-RPA calculations (*i.e.*,  $\rho_L = \rho_t$ , cf. eq. (7)). Within the “macroscopic” approach, one adopts collective transition densities,  $\rho_{coll}$ , which are assumed to have energy-independent radial shapes and are obtained from the ground-state density using a collective model. We stress that for a proper comparison between experimental and theoretical results for  $S(E)$ , one should adopt the “microscopic” folding model approach in the DWBA calculations of  $\sigma(E)$ .

## 3 Results and discussion

### 3.1 Consequences of the violation of self-consistency

Recently, the effects of common violations [26] of self-consistency in HF-RPA calculations of  $S(E)$  and  $\rho_t$  of

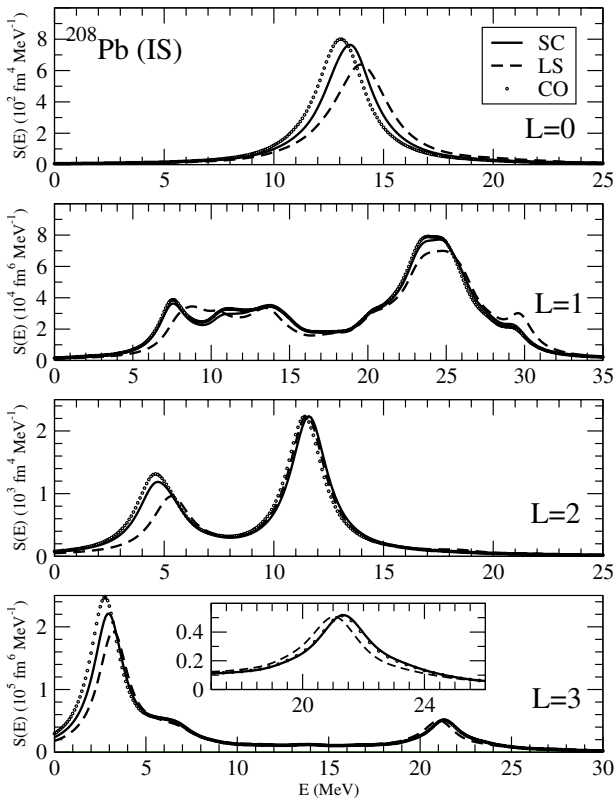


**Fig. 1.** Isoscalar strength functions of  $^{208}\text{Pb}$  for  $L = 0-3$  multipolarities are displayed. SC (full line) corresponds to the fully self-consistent calculation, whereas LS (dashed line) and CO (dotted line) represent the calculations without the residual spin-orbit and Coulomb interactions in the RPA, respectively. The interaction SGII [56] was used (taken from [54]).

various giant resonances were investigated in detail, see for example refs. [39–41, 52–54]. To demonstrate the importance of carrying out fully self-consistent calculations, we present in fig. 1 recent results for  $S(E)$  of isoscalar giant resonances in  $^{208}\text{Pb}$  with multipolarities  $L = 0-3$  using the fully self-consistent method described in refs. [36, 55]. The interaction SGII [56] was used. It is seen (see also ref. [54]) from fig. 1 that the effects of violation of self-consistency due to the neglect of the particle-hole ( $p-h$ ) spin-orbit or Coulomb interactions in the RPA calculations are most significant for the ISGMR. For the ISGMR in  $^{208}\text{Pb}$  the shift in the centroid energy  $E_0$  is about 0.8 MeV, which is 3 times larger than the experimental uncertainty. This is in agreement with fig. 1 of ref. [13], where a similar shift for  $E_{-1}$  has been obtained by means of CHF calculations.

We note that a shift of 0.8 MeV in  $E_0$  correspond to a shift of about 25 MeV in  $K$ . In fact, this shift completely solves the issue of the previously advocated disagreement between values of  $K$  extracted from Skyrme and Gogny calculations. Fully self-consistent Skyrme calculations employing existing parametrizations do not point any more to the value of about 210 MeV quoted in the introduction, but to about 235 MeV in clear agreement with the Gogny-based extraction of  $K$ .

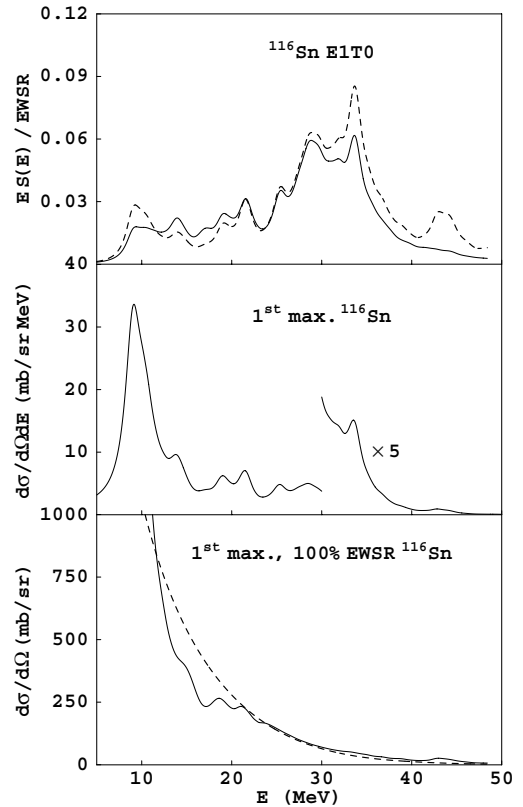


**Fig. 2.** Reconstruction of the ISGDR EWSR in  $^{116}\text{Sn}$  from the inelastic  $\alpha$ -particle cross-section. Middle panel: maximum double differential cross section obtained from  $\rho_t$  (RPA). Lower panel: maximum cross-section ( $0^\circ$ ) obtained with  $\rho_{coll}$  (dashed line) and  $\rho_t$  (solid line) normalized to 100% of the EWSR. Upper panel: the solid and dashed lines are the ratios of the middle panel curve with the solid and dashed lines of the lower panel, respectively (taken from ref. [26]).

### 3.2 Nuclear compressibility from ISGMR and ISGDR

In contrast with the ISGMR, which presents a single peak, as a rule, in heavy nuclei, the dipole response displays a low-lying, fragmented part which lies below the giant resonance. This is a systematic feature of experimental and theoretical results in a number of isotopes. Different theoretical calculations [47, 57] agree in indicating that the low-lying strength is not collective. In fact, while the centroids of the high-energy region, if calculated with interactions associated with different values of  $K$ , scale with these values, the centroids of the low-energy region do not. As far as the giant resonance centroid is concerned, discrete and continuum [58] RPA results are in good agreement with each other in  $^{208}\text{Pb}$ . Coupling with  $2ph$ -type configurations is in this case relevant, as it shifts the centroid downwards by 1 MeV (leading to good agreement with experimental data) and produces a conspicuous spreading width of about 6 MeV [59].

In refs. [26, 60], numerical calculations were carried out for the  $S(E)$ ,  $\rho_t(r)$  within the HF-RPA theory and for  $\sigma(E)$  as well, using the FM-DWBA method. The SL1 Skyrme interaction [61], which is associated with

**Table 1.** Fully self-consistent HF-RPA results [54] for the ISGDR centroid energy (in MeV) in  $^{90}\text{Zr}$  and  $^{208}\text{Pb}$ , obtained using the interactions SGII [56] and SK255 [34], compared with the RRPAs results obtained [19] with the NL3 interaction [62]. Also given are the values of  $K$ , and of the symmetry energy at saturation,  $J$ . The range of integration  $\omega_1$ – $\omega_2$  is given in the second column. The experimental data are from ref. [10] (a), ref. [11] (b), ref. [12] (c) and ref. [63] (d).

Nucleus	$\omega_1$ – $\omega_2$	Experiment	NL3	SGII	SK255
$^{90}\text{Zr}$	18–50	$25.7 \pm 0.7^a$	32.0	28.8	29.2
		$26.7 \pm 0.5^b$			
		$26.9 \pm 0.7^d$			
$^{208}\text{Pb}$	16–40	$19.9 \pm 0.8^a$	26.0	24.1	24.5
		$22.2 \pm 0.5^c$			
		$22.7 \pm 0.2^d$			
$K$ (MeV)			272	215	255
$J$ (MeV)			37.4	26.8	37.4

$K = 230$  MeV, was employed. The density-dependent Gaussian  $\alpha$ -nucleon interaction discussed in sect. 2.2 was used with parameters adjusted to reproduce the elastic cross-section, with  $\rho_0$  taken from the HF calculations. In fig. 2, we present the results of this microscopic calculation of the fraction of the energy-weighted sum rule, and the excitation cross-section  $\sigma(E)$  of the ISGDR in  $^{116}\text{Sn}$  by 240 MeV  $\alpha$ -particle scattering. It is seen from the upper panel that the use of the collective model transition densities  $\rho_{coll}$  in the whole energy range increases the EWSR by about 15%. However, the shift in the centroid energy is small (a few percents), similar in magnitude to the current experimental uncertainties. It was first pointed out in [26] that an important result of the calculation is that the maximum cross-section for the ISGDR decreases strongly at high energy and may drop below the experimental sensitivity for excitation energies above 30 MeV. This high excitation energy region contains about 20% of the EWSR. This missing strength leads to a reduction of about 3.0 MeV in the ISGDR energy which can significantly affect the comparison between theory and experiment.

In table 1, we give the results of fully self-consistent HF-RPA calculations for the ISGDR centroid energy ( $E_1$ ) obtained (see ref. [54]) using the SGII [56] and SK255 [34] interactions and compare them with the RMF-based RPA results of ref. [57] for the NL3 interaction [62] and with the experimental data. The SGII result in  $^{208}\text{Pb}$  compares well with 23.9 MeV obtained using discrete RPA in ref. [47] and with 23.4 MeV obtained using continuum RPA in ref. [48]. Note that the HF-RPA values for  $E_1$  are larger than the corresponding experimental values of the early measurements of refs. [10, 27, 28, 30] by more than 3 MeV. The more recent results of refs. [11, 12, 63, 64], seem to better agree.

### 3.3 Nuclear compressibility in relativistic and non-relativistic models

To properly compare between the predictions of the relativistic and the non-relativistic models, parameter sets

**Table 2.** The same as table 1 for the ISGMR. Experimental data are taken from refs. [11, 12].

Nucleus	$\omega_1$ – $\omega_2$	Experiment	NL3	SGII	SK255
$^{90}\text{Zr}$	0–60		18.7	17.9	18.9
	10–35	$17.81 \pm 0.30$		17.9	18.9
$^{208}\text{Pb}$	0–60		14.2	13.6	14.3
	10–35	$13.96 \pm 0.20$		13.6	14.4

for Skyrme interactions were generated in ref. [34] by a least-square fitting procedure using exactly the same experimental data for the bulk properties of nuclei considered in ref. [62] for determining the NL3 parameterization of the effective Lagrangian used in the relativistic mean-field (RMF) models. The center-of-mass correction to the total binding energy, finite-size effects of the protons and Coulomb energy were calculated in a way similar to that employed in determining the NL3 parameter set in ref. [62]. Further, the values of the symmetry energy at saturation ( $J$ ) and the charge rms radius of the  $^{208}\text{Pb}$  nucleus were constrained to be very close to 37.4 MeV and 5.50 fm, respectively, as obtained with the NL3 interaction, and  $K$  was fixed in the vicinity of the NL3 value of  $K = 271.76$  MeV. In particular, the Skyrme interactions SK272 and SK255, having  $K = 272$  and 255 MeV, respectively, were generated in ref. [34]. It is seen from table 2 that the new Skyrme interaction SK255 yields for the ISGMR centroid energies ( $E_0$ ) values which are close to the RRPAs results obtained for the NL3 interaction, in good agreement with experimental data.

To better understand this result, a more systematic analysis has been made in ref. [35], in which a larger set of new Skyrme forces has been generated, built with the same protocol used for the Lyon forces [65] and spanning a wide range of values for  $K$ , for the symmetry energy at saturation and its density dependence. The main conclusions reached in that work are the following. The ISGMR energies, calculated by means of CHF, and consequently the extracted value of  $K$ , depend on a well-defined parameter ( $K_{sym}$ ) which controls the slope of the symmetry energy curve as a function of density. The Skyrme forces having a density dependence characterized by an exponent  $\alpha = 1/6$ , like SLy4, predict  $K$  around 230–240 MeV. If this exponent is increased to values of the order of  $1/3$ , and consequently the slope of the symmetry energy curve is made stiffer, one can produce forces which are compatible with  $K$  around 250–260 MeV. This result, obtained within the framework of a different protocol for fitting the Skyrme parameters, is nonetheless in full agreement with the result of [34]. The main results of ref. [35] are shown in fig. 3. It has to be noted that a further increase of  $\alpha$ , and accordingly of  $K$ , would become difficult to obtain since the effective mass  $m^*$  would become too small.

One thus can make the clear and strong conclusion that the difference in the values of  $K$  obtained in the relativistic and non-relativistic models is not due to model dependence. It is mainly due to the different behavior of the symmetry energy within these models (cf. also [66]).

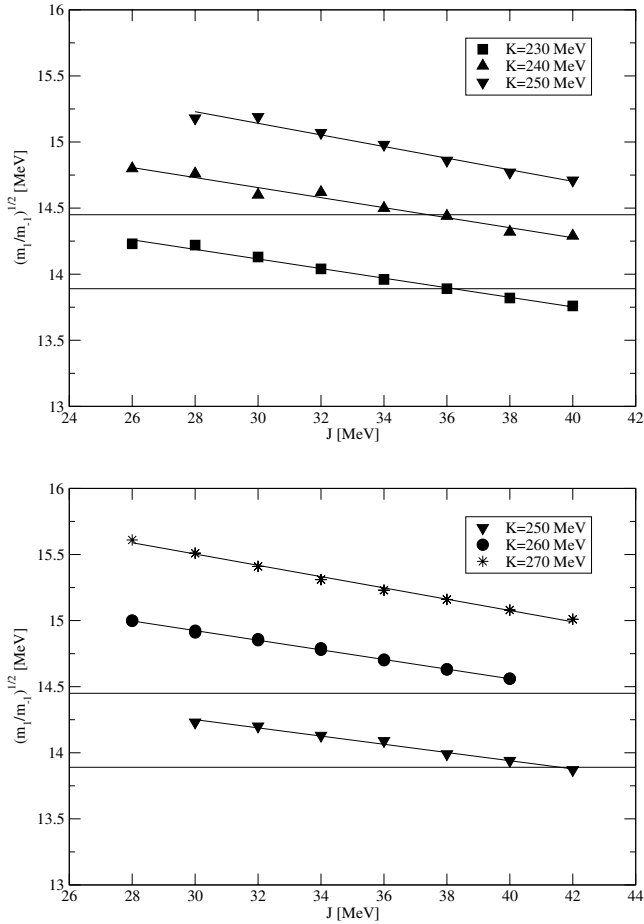


**Fig. 3.** Constrained ISGMR energies  $E_{-1}$  in  $^{208}\text{Pb}$  obtained by using the Skyrme forces built in ref. [35], and having  $\alpha = 1/6$  (upper panel) or  $\alpha = 0.3563$  (lower panel). The two horizontal lines denote the experimental upper and lower bounds. See the text for a discussion (figure taken from ref. [35]).

## 4 Conclusions

Considering the status of determining the value of the nuclear-matter incompressibility coefficient,  $K$ , from data on the compression modes ISGMR and ISGDR of nuclei, we conclude that:

i) Recent improvement in the experimental techniques led to the identification of the ISGMR in light and medium nuclei and the observation of the ISGDR in nuclei. Currently, the centroid energy  $E_0$  of the ISGMR can be deduced with very small experimental uncertainty of about 0.2 MeV, which corresponds to an uncertainty of about 7 MeV in the extracted value of  $K$ .

ii) Violations of self-consistency in HF-RPA calculations of the strength functions of giant resonances result in shifts in the calculated values of the centroid energies which may be larger in magnitude than the current experimental uncertainties. Thus, it is important to carry out fully self-consistent HF-RPA calculations in order to extract an accurate value of  $K$  from experimental data on the ISGMR and ISGDR. In fact, the prediction of  $K$  lying in the range 210–220 MeV were coming from not fully self-

consistent Skyrme calculations. Correcting for this drawback, Skyrme parametrizations of the SLy4 type predict values of  $K$  in the range 230–240 MeV.

iii) It is possible to build *bona fide* Skyrme forces so that the incompressibility is close to the relativistic value, namely 250–270 MeV.

iv) Therefore, from the ISGMR experimental data the conclusion can be drawn that  $K = 240 \pm 20$  MeV. The uncertainty of about 20 MeV in the value of  $K$  is mainly due to the uncertainty in the value of the overall shape of the nuclear-matter symmetry energy curve, as a function of density.

v) The ISGDR data tend to point to lower values for  $K$ . However, there is consensus that the extraction of  $K$  is in this case more problematic for different reasons. In particular, the maximum cross-section for the ISGDR decreases very strongly at high excitation energy and may drop below the current experimental sensitivity for excitation energies above 30 and 26 MeV for  $^{116}\text{Sn}$  and  $^{208}\text{Pb}$ , respectively. More accurate experimental data, and analysis, on the ISGDR are very much needed.

This work was supported in part by the US National Science Foundation under Grant No. PHY-0355200 and the US Department of Energy under the Grant No. DOE-FG03-93ER40773. The authors would like to acknowledge the large benefit from either discussions or collaborations with B.K. Agrawal, V.K. Au, K. Bennaceur, P. Bonche, P.F. Bortignon, M. Centelles, H. Clark, S. Fracasso, U. Garg, I. Hamamoto, A. Kolomiets, Y.-W. Lui, J. Meyer, Nguyen Van Giai, J. Piekarewicz, M.R. Quaglia, P.-G. Reinhard, P. Ring, H. Sagawa, H. Sakaguchi, A.I. Sanzhur, T. Sil, M. Uchida, D. Vretenar and D. Youngblood.

## References

1. N.K. Glendenning, Phys. Rev. C **37**, 2733 (1988).
2. W.D. Myers, W.J. Swiatecki, Phys. Rev. C **57**, 3020 (1998).
3. L. Satpathy, V.S.U. Maheswari, R.C. Nayak, Phys. Rep. **319**, 85 (1999).
4. W. Von Oertzen, H.G. Bohlen, D.T. Khoa, Nucl. Phys. A **722**, 202c (2003).
5. J.B. Natowitz, K. Hagel, Y. Ma, M. Murray, L. Qin, R. Wada, J. Wong, Phys. Rev. Lett. **89**, 21270 (2002).
6. A. Bohr, B.M. Mottleson, *Nuclear Structure II* (Benjamin, New York, 1975).
7. S. Stringari, Phys. Lett. B **108**, 232 (1982).
8. S. Shlomo, G.F. Bertsch, Nucl. Phys. A **243**, 507 (1975); K.F. Liu, Nguyen Van Giai, Phys. Lett. B **65**, 23 (1976).
9. S. Shlomo, D.H. Youngblood, Phys. Rev. C **47**, 529 (1993), and references therein; cf. also M. Pearson, Phys. Lett. B **271**, 12 (1991).
10. H.L. Clark, Y.W. Lui, D.H. Youngblood, Phys. Rev. C **63**, 031301 (2001) and references therein.
11. D.H. Youngblood, H.L. Clark, Y.W. Lui, Phys. Rev. C **69**, 034315 (2004).
12. D.H. Youngblood, H.L. Clark, Y.W. Lui, Phys. Rev. C **69**, 054312 (2004).
13. G. Colò, Nguyen Van Giai, Nucl. Phys. A **731**, 15c (2004).

14. A.A. Abrikosov, I.M. Khalatnikov, Rep. Prog. Phys. **22**, 329 (1959).
15. A. Kolomiets, V.M. Kolomietz, S. Shlomo, Phys. Rev. C **59**, 3139 (1999).
16. D. Vautherin, D.M. Brink, Phys. Rev. C **5**, 626 (1972); M. Beiner *et al.*, Nucl. Phys. A **238**, 29 (1975).
17. G.F. Bertsch, S.F. Tsai, Phys. Rep. **18**, 125 (1975).
18. J.P. Blaizot, J.F. Burger, J. Dechargé, N. Girod, Nucl. Phys. A **591**, 435 (1995).
19. Nguyen Van Giai, P.F. Bortignon, G. Colò, Zhongyu Ma, M.R. Quaglia, Nucl. Phys. A **687**, 44c (2001).
20. G.F. Bertsch, P.F. Bortignon, R.A. Broglia, Rev. Mod. Phys. **55**, 287 (1983).
21. C. Mahaux, P.F. Bortignon, R.A. Broglia, C.H. Dasso, Phys. Rep. **120**, 1 (1985).
22. P.-G. Reinhard, C. Toepffer, Int. J. Mod. Phys. E **3**, 435 (1994).
23. G. Colò, P.F. Bortignon, N. Van Giai, A. Bracco, R.A. Broglia, Phys. Lett. B **276**, 279 (1992).
24. N. Marty *et al.*, Nucl. Phys. A **230**, 93 (1975); M.N. Harakeh *et al.*, Phys. Rev. Lett. **38**, 676 (1977); D.H. Youngblood *et al.*, Phys. Rev. Lett. **39**, 1188 (1977).
25. J.P. Blaizot, Phys. Rep. **64**, 171 (1980).
26. S. Shlomo, A.I. Sanzhur, Phys. Rev. C **65**, 044310 (2002); S. Shlomo, Pramana J. Phys. **57**, 557 (2001).
27. H.P. Morsch, M. Rogge, P. Turek, C. Mayer-Böricke, Phys. Rev. Lett. **45**, 337 (1980).
28. C. Djalali, N. Marty, M. Morlet, A. Willis, Nucl. Phys. A **380**, 42 (1982).
29. T.S. Dumitrescu, F.E. Serr, Phys. Rev. C **27**, 811 (1983).
30. B. Davis *et al.*, Phys. Rev. Lett. **79**, 609 (1997).
31. Zhong-yu Ma, Nguyen Van Giai, A. Wandelt, D. Vretenar, Nucl. Phys. A **686**, 173 (2001).
32. D. Vretenar, T. Nikšić, P. Ring, Phys. Rev. C **68**, 024310 (2003).
33. T. Nikšić, D. Vretenar, P. Ring, Phys. Rev. C **66**, 064302 (2002).
34. B.K. Agrawal, S. Shlomo, V.K. Au, Phys. Rev. C **68**, 031304(R) (2003); S. Shlomo, B.K. Agrawal, V.K. Au, Nucl. Phys. A **734**, 589 (2004).
35. G. Colò, Nguyen Van Giai, J. Meyer, K. Bennaceur, P. Bonche, Phys. Rev. C **70**, 024307 (2004).
36. P.-G. Reinhard, Ann. Phys. (Leipzig) **1**, 632 (1992).
37. T. Nakatsukasa, K. Yabana, Phys. Rev. C **71**, 024301 (2005).
38. O. Bohigas, A.M. Lane, J. Martorell, Phys. Rep. **51**, 267 (1979).
39. J. Terasaki, J. Engel, M. Bender, J. Dobaczewski, W. Nazarewicz, M. Stoitsov, Phys. Rev. C **71**, 034310 (2005).
40. B.K. Agrawal, S. Shlomo, A.I. Sanzhur, Phys. Rev. C **67**, 034314 (2003).
41. B.K. Agrawal, S. Shlomo, Phys. Rev. C **70**, 014308 (2004).
42. J. Piekarewicz, Phys. Rev. C **62**, 051304 (2000).
43. M.L. Gorelik, S. Shlomo, M.H. Urin, Phys. Rev. C **62**, 044301 (2000).
44. A. Kolomiets, O. Pochivalov, S. Shlomo, *Progress in Research, April 1, 1998 - March 31, 1999* (Cyclotron Institute, Texas A&M University, 1999) III-1.
45. G.F. Bertsch, Suppl. Prog. Theor. Phys. **74**, 115 (1983).
46. Nguyen Van Giai, H. Sagawa, Nucl. Phys. A **371**, 1 (1981).
47. G. Colò, Nguyen Van Giai, P.F. Bortignon, M.R. Quaglia, Phys. Lett. B **485**, 362 (2000).
48. I. Hamamoto, H. Sagawa, Phys. Rev. C **66**, 044315 (2002).
49. V.I. Abrosimov, A. Dellafiore, F. Matera, Nucl. Phys. A **697**, 748 (2002).
50. G.R. Satchler, *Direct Nuclear Reactions* (Oxford University Press, Oxford, 1983).
51. G.R. Satchler, D.T. Khoa, Phys. Rev. C **55**, 285 (1997).
52. S.A. Fayans, E.L. Trykov, D. Zawischa, Nucl. Phys. A **568**, 523 (1994).
53. S. Péru, J.F. Berger, P.F. Bortignon, Eur. Phys. J. A **26**, 25 (2005).
54. T. Sil, S. Shlomo, B.K. Agrawal, P.-G. Reinhard, Phys. Rev. C **73**, 034316 (2006).
55. P.-G. Reinhard, Nucl. Phys. A **646**, 305c (1999).
56. Nguyen Van Giai, H. Sagawa, Phys. Lett. B **106**, 379 (1981).
57. D. Vretenar, A. Wandelt, P. Ring, Phys. Lett. B **487**, 334 (2000).
58. I. Hamamoto, H. Sagawa, X.Z. Zhang, Phys. Rev. C **57**, R1064 (1998).
59. G. Colò, Nguyen Van Giai, P.F. Bortignon, M.R. Quaglia, *Proceedings of the RIKEN Symposium on Selected Topics in Nuclear Collective Excitations, RIKEN, Wako City 1999*, RIKEN Rev. **23**, 39 (1999).
60. A. Kolomiets, O. Pochivalov, S. Shlomo, Phys. Rev. C **61**, 034312 (2000).
61. K.-F. Liu, H.-D. Lou, Z.-Y. Ma, Q.-B. Shen, Nucl. Phys. A **534**, 1; 25 (1991).
62. G.A. Lalazissis, J. König, P. Ring, Phys. Rev. C **55**, 540 (1997).
63. M. Uchida *et al.*, Phys. Rev. C **69**, 051301 (2004).
64. M. Itoh *et al.*, Phys. Rev. C **68**, 064602 (2003).
65. E. Chabanat, P. Bonche, P. Haensel, J. Meyer, R. Schaeffer, Nucl. Phys. A **627**, 710 (1997); **635**, 231 (1998).
66. J. Piekarewicz, Phys. Rev. C **66**, 034305 (2002).